Published in final edited form as:
J Immunol. 2012 June 15; 188(12): 6135–6144. doi:10.4049/jimmunol.1103487.

The Cytoskeletal Adaptor Protein IQGAP1 Regulates TCR-mediated Signaling and F-actin Dynamics[1]

Jacquelyn A. Gorman[*], **Alexander Babich**[†], **Christopher J. Dick**[*], **Renee A. Schoon**[*], **Alexander Koenig**[‡], **Timothy S. Gomez**[*,‡], **Janis K. Burkhardt**[†], and **Daniel D. Billadeau**[*,‡,2]

[*]Department of Immunology, Schulze Center for Novel Therapeutics, College of Medicine, Mayo Clinic, Rochester, MN, 55901

[‡]Division of Oncology Research, Schulze Center for Novel Therapeutics, College of Medicine, Mayo Clinic, Rochester, MN, 55901

[†]Department of Pathology and Laboratory Medicine, Children's Hospital of Philadelphia and Perelman School of Medicine, University of Pennsylvania, Philadelphia, PA 19104

Abstract

The Ras GTPase-activating-like protein IQGAP1 is a multi-modular scaffold that controls signaling and cytoskeletal regulation in fibroblasts and epithelial cells. However, the functional role of IQGAP1 in T cell development, activation and cytoskeletal regulation has not been investigated. Herein, we show that IQGAP1 is dispensable for thymocyte development, as well as microtubule organizing center polarization and cytolytic function in $CD8^+$ T cells. However, IQGAP1-deficient $CD8^+$ T cells, as well as Jurkat T cells suppressed for IQGAP1 were hyper-responsive, displaying increased IL-2 and IFN-γ production, heightened LCK activation, and augmented global phosphorylation kinetics following TCR ligation. Additionally, IQGAP1-deficient T cells exhibited increased TCR-mediated F-actin assembly and amplified F-actin velocities during spreading. Moreover, we found that discrete regions of IQGAP1 regulated cellular activation and F-actin accumulation. Taken together, our data suggest that IQGAP1 acts as a dual negative regulator in T cells, limiting both TCR-mediated activation kinetics and F-actin dynamics via distinct mechanisms.

Keywords

F-actin; T cell activation; IQGAP1; cytotoxicity; MTOC

Introduction

A productive interaction between a T cell and an APC bearing an appropriate MHC- peptide complex results in accumulation of F-actin and polarization of the microtubule organizing center (MTOC)[3] toward the T cell – APC contact site, known as the immunological synapse

[1]This work was supported in part by an Immunology Predoctoral Training grant NIH-T32-AI07425 (J.A.G.), Allergic Diseases Training grant NIH-T32-AI07047 (T.S.G.) and NIH grant R01-AI065474 (D.D.B.). D.D.B. is a Leukemia and Lymphoma Society Scholar.

[2]Address correspondence and email requests to Dr. Daniel Billadeau, Department of immunology and Division of Oncology Research, Mayo Clinic College of Medicine, Rochester, MN 55905, USA. billadeau.daniel@mayo.edu.

Disclosures
The authors have no financial conflict of interest.

[3]Abbreviations used in this paper: APC, antigen presenting cell; IS, immunological synapse; MTOC, microtubule organizing center; GRD, GTPase related domain; GAP, GTPase activating protein; CHD, calponin homology domain; DN, double negative.

(IS) (1, 2). These cytoskeletal changes are essential for proper APC recognition, IS formation, and efficient signaling leading to T cell activation (2). Numerous signaling proteins that function downstream of the TCR are intimately involved in the molecular pathways contributing to reorganization of the F-actin and microtubule cytoskeletons, yet the mechanisms by which many of these proteins are recruited, and how they exert their actin- and microtubule-regulating activities is, for the most part, unresolved.

F-actin reorganization was shown through the use of pharmacological agents to be essential for T cell activation (1, 3, 4). MTOC polarization toward the IS is also thought to be F-actin dependent (5). Several cytoskeletal interacting proteins including Vav1, HS1, mDia1, WAVE2, and WASP, have been identified as participants in cytoskeletal reorganization and signaling during T cell – APC interaction (2, 6–12). Despite this knowledge, there are still many unanswered questions about how the cytoskeleton modulates TCR signaling. Additionally, whether other proteins participate in these processes independently of the known cytoskeletal regulators, or in concert with them, remains to be determined.

One family of adaptor proteins, the IQGAP family, has been linked to both the microtubule and actin cytoskeletal networks in several cell types (13). The IQGAP family consists of three highly homologous isoforms (IQGAP1, 2, and 3). Whereas IQGAP1 is ubiquitously expressed, IQGAP2 and IQGAP3 have more distinct expression patterns (14). IQGAP proteins are multi-modular, consisting of a calponin homology domain (CHD) at the N-terminus, followed by a poly-proline binding WW domain, four tandem IQ motifs that bind calmodulin, a RasGAP-related domain (GRD), and a RasGAP-containing domain at the C-terminus (15, 16). The domains of IQGAP1 have been shown to mediate numerous protein – protein interactions. In fact, the WW domain was found to interact with ERK1 and ERK2, whereas the IQ domains can bind MEK1, MEK2, and B-RAF, suggesting the possibility that IQGAP1 may regulate activation of the Ras-MAPK signaling cascade (17–19). Instead of accelerating the intrinsic GTPase activity of Cdc42 and Rac1, the GAP domains of IQGAP proteins keep them in their active GTP-bound state (20–22). In epithelial cells, IQGAP1 was shown to regulate E-cadherin mediated cell-cell adhesion, polarity, motility, proliferation, and MAP kinase signaling (17, 18, 23–30). Thus, IQGAP1 has the capacity to integrate multiple signaling cascades downstream of cell surface receptors.

In addition to functioning as a signaling adaptor protein, IQGAP1 was recently shown to bind the barbed ends of F-actin in a calmodulin-regulated manner and to display actin-capping activity through its C-terminus *in vitro* (31). IQGAP1 also binds to regulators of the actin cytoskeleton including N-WASP through its GRD and mDia1 via its RasGAP domain (32, 33). Additionally, IQ domains of IQGAP1 interact with the actin-based motor myosin via the essential light chain (34), and the RasGAP domain of IQGAP1 binds the microtubule-associated protein, CLIP-170 (35). Consequently, IQGAP1 has been suggested to function as a facilitator of communication between the F-actin and microtubule networks (35, 36). In fact, Stinchcombe and Griffiths demonstrated that IQGAP1 localizes to the F-actin-rich region of the cytolytic synapse formed between a $CD8^+$ T cell and target cell (5), and based on this cellular localization, suggested that IQGAP1 might coordinate F-actin and microtubules during cellular cytotoxicity. However, one study has suggested that these two systems can be separated (37). Therefore, the exact role of IQGAP1 in regulating the interplay between the cytoskeletal systems and signaling during T cell development and activation needs to be investigated. Also, functional consequences of direct F-actin regulation by IQGAP1 have not been well characterized. So far, there is no *in vivo* evidence to support the recent suggestion that IQGAP1 has actin-capping activity, so its functional role in actin recruitment/stabilization at the IS is also of interest.

To address these issues, we have utilized IQGAP1-deficient mice, as well as shRNA-mediated knockdown in the Jurkat T cell model. We find that thymocyte development was unaltered in IQGAP1 knockout mice, and IQGAP1 was surprisingly dispensable for MTOC polarization and cellular cytotoxicity. However, IQGAP1-deficient T cells showed increased cytokine production, enhanced LCK activation and heightened phosphorylation kinetics following TCR ligation. In addition, they displayed augmented F-actin accumulation upon TCR ligation and enhanced kinetics of TCR-mediated F-actin retrograde flow. Interestingly, expression of the N-terminus of IQGAP1 could partially rescue F-actin accumulation and IL-2 gene transcription, whereas the increased F-actin dynamics could be fully reversed by rescue with the F-actin capping C-terminus of IQGAP1. Based on these results, we propose that IQGAP1 is a critical modulator of T cell activation that regulates TCR-mediated signaling and F-actin dynamics through distinct molecular mechanisms.

Materials and Methods

Reagents and Plasmids

Antibodies against ZAP-70 and LCK have been previously described (38, 39). Anti-phosphoSrc and anti-ERK2 were from Cell Signaling Technology. Anti-IQGAP1 was obtained by immunization of rabbits with a KLH-conjugated synthetic peptide corresponding to amino acids 2–25 of mouse IQGAP1 (Colcalico Biologicals Inc). Anti-IQGAP2, and anti-phosphotyrosine (4G10) were from Upstate Biotechnology/Millipore. Anti-γ-Tubulin was from Sigma-Aldrich. The anti-human CD3 (OKT3) was purchased from the Mayo Pharmacy and anti-human CD28 from (BD Biosciences). The anti-mouse CD3 (2C11) and CD28 (37.51) were purchased from Bio-X-Cell. The Mayo Peptide Synthesis Facility generated the SIINFEKL (SIN) and RAHYNIVTF (E7) peptides. The altered peptide ligands Q4R7 (SIIQFERL), Q4H7 (SIIQFEHL), and pG4 (SIIGFEKL) were a gift from Dr. Diana Gil Pages (Mayo Clinic)(Elim Biopharmaceu, Inc.)(40). The shRNA suppression vectors pFRT.H1p, pCMS3.cherry.H1p, and pCMS4.eGFP.H1P have been previously described (12, 41, 42). The shIQGAP1 targeting sequence (5′-GTCCTGAACATAATCTCAC-3′) corresponds to nucleotides 1318–1336 using NCBI Genbank Accession number NM_003870 (http://www.ncbi.nlm.nih.gov/genbank/). The IQGAP1 cDNA was made shRNA-resistant using PCR-based site-directed mutagenesis (5′-CCgGAgCAcAATCTCAC-3′).

Cell Culture and Isolation

Jurkat T cells were passaged as previously described (12). The P815 cell line was described (43). The EL-4 mouse lymphoma cell line was cultured in 5% FBS, 5% BCS and 1% L-Glutamine. To generate primary mouse T cells, splenocytes were dissociated, and RBCs were lysed with ACK solution (155 mM ammonium chloride, 1 mM potassium bicarbonate and 0.1 mM EDTA disodium salt). Mouse $CD4^+$ and $CD8^+$ T cells were negatively isolated using MACs Isolation Kit II (Milteny). $CD4^+$ T cells were cultured in RPMI, 1% non-essential amino acids, 1% L-Glutamine, 1% sodium pyruvate, 0.05% 2-ME, and 10% FBS. $CD8^+$ T cells were cultured in RPMI, 1% non-essential amino acids, 1% L-Glutamine, 1% sodium pyruvate, 0.05% 2-ME, 3% Fetal bovine serum and 20 units/ml of IL-2.

Jurkat T Cell Transfection, Stimulation, and Western blotting

Jurkat T cells were transiently transfected using a BTX ECM830 electroporator (315 V, 10 msec, 1 pulse). 40 μg of each suppression plasmid or 50–60 μg of suppression/re-expression plasmids were used in each transfection, and experiments were conducted 72 hours post transfection. Jurkat T cells were stimulated with 5–10 μg of anti-CD3/CD28 and cross-linked with goat-anti-mouse Ig (Cappell/MP Biomedicals).

Mice

IQGAP1$^{-/-}$ mice (44) were obtained from Dr. Wadie Bahou (SUNY at Stonybrook). Sex-matched littermates were used in all experiments unless indicated. In order to generate IQGAP1-deficient OT-I TCR transgenic mice, IQGAP1$^{-/-}$ mice were bred to homozygous OT-I TCR transgenic mice and heterozygous progeny were then bred to generate the experimental animals. All mice were genotyped for the presence of the Vα2, Vβ5 TCR transgene, and for deletion of the IQGAP1 gene. Immunoblotting to demonstrate loss of IQGAP1 and flow cytometry for expression of Vα2 and Vβ5 was performed to confirm TCR transgene expression. All mice were between 5 and 40 weeks of age. All animal work complied with Mayo Clinic's guidelines and was approved by the Institutional Animal Care and Use Committee.

Cytotoxicity Assays

P815 cells were stained with anti-CD3/CD28 and mixed with splenic CD8$^+$ T cells. Splenic OT-I T cells were stimulated with 1 μg/ml of SIINFEKL for 48 hours and allowed to rest for 48 hours. EL-4 cells were pulsed with either 10 μg/ml of E7 peptide, SIINFEKL peptide, or an altered peptide ligand for 1 hour. Along with the peptide, these cells were loaded with ^{51}Cr 50 μCi/1×10^6 cells. EL-4 and OT-I T cells were allowed to interact for 4 hours, pelleted and the supernatant was analyzed for ^{51}Cr release as described (45).

Immunofluorescence Microscopy

Splenic OT-I T cells were stimulated with 1 μg/ml of SIINFEKL for 72 hours and allowed to rest for 24 hours. Conjugates were formed with EL-4 cells pre-pulsed with either E7 peptide or SIINFEKL peptide. CD8$^+$ T cells and EL-4 cells were allowed to interact for 30 minutes for F-actin or 20 minutes for MTOC polarization at 37°C. Conjugates were spread onto poly-L-lysine-coated coverslips for 5 minutes at 37°C. Cells were fixed and stained for F-actin and α-tubulin as previously described (46) and imaged on a Zeiss LSM-710 confocal or Zeiss Axiovert 200M microscope. Quantification of F-actin accumulation or MTOC polarization at the IS was done as previously described (42). At least 50 conjugates were analyzed in each of three experiments. Quantification of the intensity of polarized F-actin was determined by Zen software. Pixel intensities were broken into 3 groups and percentages of cells in each group are shown. At least 60 conjugates were analyzed in total. Data represent average ±SD.

Flow cytometry

All antibodies were from BD Biosciences or eBiosciences. All samples were run on either BD FACSCanto II or BD LSR II. Jurkat T cells were stimulated for 1 or 5 minutes with CD3/CD28. The cells were fixed with 4% paraformaldehyde (Electron Microscopy Sciences) and permeabilized with 0.15% Surfact-Amps X-100 (Thermo Scientific). F-actin was labeled with either FITC- or AlexaFluor647-conjugated phalloidin (Invitrogen). Stimulation time points were labeled in triplicate and repeated in three different experiments. Statistical significance was determined using a two-tailed Student's t test.

ELISA and Quantitative RT-PCR

For ELISA and RT-PCR, CD4$^+$ T cells were stimulated for 24 hours with the indicated concentrations of anti-CD3 and anti-CD28. IL-2 levels in the supernatants were analyzed by ELISA (Ebiosciences). Quantitative analysis of mRNA expression was performed as previously described (47). Briefly, T cells were stimulated with the indicated concentrations of antibody over time, and RNA was subsequently extracted using the RNeasy Mini Kit (Qiagen). One microgram of total RNA was transcribed into cDNA using the Superscript III RT-PCR Kit (Invitrogen) according to the manufacturer's instructions. Quantitative PCR

was performed using the comparative CT method with the SYBR Green PCR Master Mix (Applied Biosystems) and the ABI Prism 7900TM Sequence Detection System. Experiments were performed in triplicate using independently generated cDNAs. Gene specific primers for mouse and human IL-2 were designed by using software from the IDT website (http://www.idtdna.com/scitools/Applications/RealTimePCR/) and are shown below: mouse RPLP0: forward 5′-AGATCCGCATGTCCCTTC-3′, reverse 5′-CCTTGCGCATCATGGTGTT-3′; mouse IFN-γ: forward 5′-CCTAGCTCTGAGACAATGAACG-3′; reverse 5′-TTCCACATCTATGCCACTTGAG-3′; mouse IL-2: forward 5′-TGATGGACCTACAGGAGCTCCTGA-3′, reverse 5′-GAGTCAAATCCAGAACATGCCGCAG-3′; human RPLP0: forward 5′-AGATCCGCATGTCCCTCC-3′, reverse 5′-CCTTGCGCATCATGGTGTT-3′; human IL-2: forward 5′-AACTCCTGTCTTGCATTGCAC-3′, reverse 5′-GCTCCAGTTGTAGCTGTGTTT-3′.

Live-cell Imaging

Eight-well Lab-Tek II chambered cover glasses (Nunc) were prepared and coated with OKT3 (Biolegend), as described previously (48). Immediately before imaging, wells were covered with 400 μl of imaging medium (phenol red-free RPMI 1640, with 25 μM HEPES) and equilibrated to 37°C on the microscope stage within a Solent environmental chamber. Cultured cells were harvested and resuspended in imaging medium at 2×10^6/ml. Spreading was initiated by adding 10 μl of cell suspension to the well. Time-lapse series of randomly selected cells were collected on a Zeiss Axiovert 200 equipped with a 63× objective and a PerkinElmer ERS6 Ultraview spinning disk confocal system. 0.5-μm thick Z stacks of two planes were collected using an Orca ER camera (Hamamatsu) at 3-second intervals for 1–5 minutes.

Kymography and statistical analysis

Kymographs were generated along the radii of spread T cells using Volocity 6.0 software (Perkin Elmer) and analyzed for F-actin features. Velocity was determined based on the deflection angle of diagonal trajectories. Four kymographs were generated per IS and one velocity measurement was made per kymograph. Statistical analysis was performed using Microsoft Excel, with statistical significance determined using a two-tailed Student's t test for unpaired samples with equal variances.

Results

Thymocyte development and peripheral T cell numbers are normal in the IQGAP1-deficient mice

The role of IQGAP1 has been extensively studied in epithelial cells and cancer. However, the functional role of IQGAP1 in T cells remains unclear. We began our analysis by verifying that the IQGAP1 protein was absent in T cells from IQGAP1$^{-/-}$ mice (44, 49). These mice have a neomycin cassette inserted in the IQGAP1 gene locus replacing exon 27. Using an antibody against the IQGAP1 N-terminus, we found that IQGAP1 was completely absent from total thymocytes and splenic CD4$^+$ T cells (Fig. 1*A*), and a smaller truncated protein product was never observed (Supplemental Fig. S1*A*). Thus, although it was reported that IQGAP1 mRNA was found in IQGAP1$^{-/-}$ T cells (50), we could not detect intact or partial IQGAP1 protein in either thymocytes or purified splenic CD4$^+$/CD8$^+$ T cells. We conclude that any remaining RNA is likely degraded by nonsense RNA-mediated decay.

We next analyzed T cell development in the absence of IQGAP1. We found that double negative (DN), double positive (DP), and single positive (SP) thymocyte populations were unaltered in the absence of IQGAP1 (Fig. 1*B* and 1*C*). Early thymocyte progenitors, DN2, DN3 and DN4, were also unchanged compared to wild type T cells (data not shown). Additionally, there were no differences in the number of splenic or lymphatic $CD4^+$ or $CD8^+$ T cells (Fig. 1*D*). Before testing the functionality of the knockout T cells, we confirmed TCR and CD28 surface levels were normal (Fig. 1*E*). Taken together, these data indicate that the loss of IQGAP1 does not alter thymocyte development, the ability of naïve T cells to migrate into peripheral lymphoid organs, or TCR levels.

IQGAP1 does not regulate MTOC polarization or cytotoxicity

Since IQGAP1 was shown to localize to the cytolytic synapse (5), and was hypothesized to regulate T cell MTOC polarity in line with its role in epithelial cells (25), we examined T cell mediated cytotoxicity and MTOC polarization in the IQGAP1 knockout. We used $IQGAP1^{+/+}$ and $IQGAP1^{-/-}$ OT-I TCR transgenic $CD8^+$ T cells to investigate MTOC polarization to the IS and cell-mediated killing using control (E7) or antigen-loaded (SIINFEKL) EL4 cells. Consistent with our findings in non-transgenic mice, thymocyte development was normal in the OT-I mice (unpublished data). Interestingly, TCR transgenic $IQGAP1^{-/-}$ lymphocytes were able to polarize their MTOC toward the IS (Fig. 2*A* and 2*B*) and efficiently killed antigen-loaded EL4 cells (Fig. 2*C*). To confirm this result, we used an alternate system to measure cytotoxicity. Using $CD8^+$ T cells isolated from non-TCR transgenic mice, we assessed $IQGAP1^{-/-}$ T cells' ability to kill 2c11-pulsed P815 cells. Again, we saw no difference between $IQGAP1^{-/-}$and $IQGAP1^{+/+}$ killing ability (Supplemental Fig. S1*B*). To determine whether we were driving cytotoxicity as a result of over stimulating the system with a high concentration of peptide, we tested both lower concentrations and different strength agonists. Surprisingly, but consistent with the notion that IQGAP1 was not involved in TCR-driven cell-mediated cytotoxicity, we find that there is no significant difference in killing between wild type and IQGAP1-deficient OT-I T cells regardless of SIN concentration or agonist strength (Fig. 2*D*). Thus, loss of IQGAP1 does not affect T cell signaling leading to either MTOC polarization or cellular cytotoxicity.

IQGAP1-deficiency increases cytokine gene expression and signaling

Since IQGAP1 was shown to regulate the MAP kinase pathway, (17–19) we next examined the effect of depleting IQGAP1 on T cell signaling and activation. Interestingly, $IQGAP1^{-/-}$ OT-I $CD8^+$ T cells displayed increased basal tyrosine phosphorylation levels (Fig. 3*A*, compare 0 time points), and demonstrated enhanced global tyrosine phosphorylation following TCR crosslinking (Fig. 3*A*). Consistent with heightened tyrosine phosphorylation in $IQGAP1^{-/-}$ OT-I T cells, we also observed augmented IL-2 and IFN-γ mRNA levels by quantitative RT-PCR (Fig. 3*B and* 3*C*). Consistent with this result, IQGAP1-deficient T cells secreted more IL-2 and IFN-γ compared to control cells (Fig. 3*D* and 3*E*). Furthermore, $IQGAP1^{-/-}$ $CD4^+$ T cells and IQGAP1-supressed Jurkat T cells show increased IL-2 mRNA and secretion of IL-2 (Fig. 4*A*, Supplemental Fig. 2*A* and 2*B*) consistent with IQGAP1 regulating TCR signaling leading to elevated cytokine production in both mouse T cell subsets, as well as in human T cells. Taken together, these data indicate that IQGAP1 likely functions as a negative regulator or modulator of T cell signaling leading to IL-2 and IFN-γ gene transcription.

We next sought to examine at which point in the signaling cascade IQGAP1 was exerting its effect. We began our investigation using IQGAP1-suppressed Jurkat T cells since they phenocopy $IQGAP1^{-/-}$ T cells at the level of increased IL-2 gene transcription. Interestingly, IQGAP1-suppressed Jurkat T cells displayed increased global tyrosine phosphorylation levels following TCR crosslinking when compared to control cells (Fig.

4*B*). Consistent with the mouse model, we routinely observed that IQGAP1 depletion increased basal tyrosine phosphorylation (Fig. 3*A* and 4*B*, compare 0 time points) suggesting that IQGAP1 may suppress proximal kinase activation. We therefore analyzed TCR-induced LCK phosphorylation at tyrosine 394, within the kinase activation loop. Indeed, IQGAP1-suppressed Jurkat and $CD8^+$ knockout T cells showed increased TCR-mediated LCK phosphorylation at Tyr394 (Fig. 3*A* and 4*B*). As this antibody can also cross-react with FYN, we also immunoprecipitated LCK and assessed Tyr394 phosphorylation. Again we found that the kinetics and extent of phosphorylation were increased in IQGAP1-depleted Jurkat cells (Fig. 4*C*). Taken together, these data indicate that IQGAP1 regulates LCK activation following TCR ligation.

To confirm that the heighted levels of phosphorylation and IL-2 mRNA expression were a result of the loss of IQGAP1, we utilized a suppression/rescue system to reconstitute IQGAP1-suppressed Jurkat T cells with an shRNA resistant IQGAP1 cDNA (12). Importantly, re-expression of wild type IQGAP1 restored the kinetics of TCR-stimulated tyrosine phosphorylation and LCK phosphorylation to that of control transfected cells (Fig. 5*A* and 5*B*). Subsequently, we used deletion mutants (Fig. 5*A*) to examine which domains of IQGAP1 modulate TCR signaling. TCR-stimulated IL-2 mRNA levels were fully restored to that of control transfected cells following reconstitution with either IQGAP1 wild type or an N-terminal fragment of IQGAP1 encompassing amino acids 1–735 (Fig. 5*C*). In contrast to the N-terminal portion of IQGAP1, the C-terminal half of the molecule (amino acids 744–1657) did not rescue IL-2 mRNA levels. Thus the N-terminus of IQGAP1 modulates TCR-mediated activation leading to IL-2 production while the C-terminus, which has been implicated in F-actin capping (31), does not. To further investigate the role of the IQGAP1's N-terminus, we examined the phosphorylation kinetics following TCR ligation (Supplemental Fig. S2*C*). Interestingly, we found that neither the N-terminal nor the C-terminal fragments rescued tyrosine phosphorylation kinetics. Taken together, the N-terminus of IQGAP1 appears to modulate TCR-driven IL-2 gene transcription independent of its ability to regulate TCR-dependent proximal signaling (see Discussion).

IQGAP1 negatively regulates F-actin accumulation at the IS

In a recent report, IQGAP1 was shown to cap F-actin *in vitro* (31). To investigate the role of IQGAP1 in modulating F-actin dynamics in T cells, we first formed conjugates with TCR transgenic OT-I wild type or $IQGAP1^{-/-}$ T cells and SINFEKL-loaded EL-4 cells. Although the overall proportion of $IQGAP1^{-/-}$ OT-I T cells that accumulated F-actin at the IS was similar to that of control (Fig. 6*A*), the amount of F-actin that accumulated at the IS was dramatically increased without IQGAP1 (Fig. 6*B*). In fact, measuring pixel intensity at the IS, we found that there were more $IQGAP1^{-/-}$ cells with increased F-actin content at the IS compared to control cells (Fig. 6*C*). To further analyze stimulated F-actin content, we examined $IQGAP1^{-/-}$ OT-I T cells spread on 2C11-coated coverslips (Fig. 6*D*, Supplemental Fig. S3). Indeed, knockout T cells had augmented TCR-stimulated F-actin. Furthermore, the $IQGAP1^{-/-}$ T cells showed faster F-actin kinetics and prolonged spreading. Moreover, using 3D reconstruction of Z-stacks at 5 minutes post-stimulation we observed that the enhanced F-actin in $IQGAP1^{-/-}$ cells accumulated at the base of the cell (Fig. 6*D*).

We next utilized a flow cytometry-based assay to quantitate the amount of TCR-stimulated F-actin. Consistent with the qualitative and quantitative microscopic analysis of the knockout cells, IQGAP1-suppresssed Jurkat T cells showed increased F-actin following TCR ligation (Fig. 7A), whereas unstimulated baseline F-actin content was not affected (data not shown). Having observed more TCR-stimulated F-actin accumulation at the IS, we hypothesized that IQGAP1 might regulate F-actin retrograde flow during TCR signaling. To evaluate the effects of IQGAP1 knockdown on F-actin dynamics we used Jurkat T cells,

stably expressing low levels of GFP-actin (12). T cells were then imaged while spreading on an anti-CD3-coated cover glass, as described previously (51). Confocal imaging of the IS confirmed our observations of increased F-actin enrichment in the lamellipodia of T cells suppressed for IQGAP1, compared to control transfected cells (Fig. 7*B*, and Supplemental Movie 1). IQGAP1-deficient T cells also spread to a greater extent and spreading persisted longer relative to non-suppressed cells (data not shown). Furthermore, kymography showed that T cells lacking IQGAP1 had faster F-actin retrograde flow relative to the control cells (Figure 7*C* and 7*D*). The lamellipodia also occupied a larger portion of the synapse area than in control counterparts. Taken together, these data suggest that IQGAP1 regulates the extent of F-actin accumulation and the velocity of F-actin movement at the IS.

Lastly, we used suppression/re-expression studies to identify which region of IQGAP1 impacts F-actin accumulation. Significantly, TCR-stimulated F-actin levels were reduced to control levels following reconstitution with either wild type IQGAP1 or the C-terminal fragment (744–1657), that has F-actin capping potential (Fig. 7*E*). Interestingly, the region that rescued modulation of IL-2 gene transcription, IQGAP1 1–735, was capable of at least partial rescue of F-actin accumulation in this assay.

Discussion

IQGAP1 regulates signaling cascades and the cytoskeleton through its scaffolding functions (13, 52). However in this study, we show that loss of IQGAP1 does not affect MTOC polarization or cytotoxicity. Alternatively, we demonstrate that IQGAP1 normally attenuates signaling events and F-actin dynamics following TCR ligation. Specifically, we find that IQGAP1 modulates proximal TCR-mediated LCK activation leading to increased production of IL-2 and IFN-γ. Furthermore, we show that IQGAP1-deficient T cells display enhanced F-actin accumulation and increased velocity of retrograde flow at the IS. Altogether, our data suggest that IQGAP1 is a critical negative modulator of T cell activation.

IQGAP1 has been suggested to integrate crosstalk between the cytoskeletal systems, leading to MTOC polarization and cytotoxicity (5). In fact, a recent study examining the role of IQGAP1 in natural killer cells demonstrated a critical role for IQGAP1 in natural killer cell-mediated cytotoxicity (53). These results conflict with our analysis of IQGAP1-deficient $CD8^+$ T cells, which show no obvious defect in either MTOC polarization to the cytotoxic synapse or cell mediated killing. The differences might be attributable to either the use of shRNA versus a knockout model or differences in the cell types being analyzed. In fact, it has been suggested in a previous study that the requirements for granule secretion in NK cells are different (54). The delivery of lytic granules to the NK IS is through small areas devoid of F-actin however there is still a need for Myosin IIA (54, 55). On the contrary, previous work has suggested that actin is not a barrier for granule secretion in cytotoxic T lymphocytes (5, 56). These differences could explain the conflicting observed phenotypes. Our results suggest that neither MTOC polarization nor cytotoxicity is affected in $CD8^+$ T cells completely lacking IQGAP1.

The T cell cytoskeleton acts as a crucial platform for T cell signaling and ultimately T cell activation. Previous studies have shown that both F-actin and the microtubule cytoskeleton are needed for proper IS formation, TCR signaling, and T cell activation (57). However, the exact functions of F-actin in TCR signaling remain unclear. Recent reports suggest that F-actin dynamics may modulate TCR function by exerting physical forces on signaling complexes or microcluster biogenesis (57, 58)(AB and JKB unpublished observations). Although this is not the only possible explanation for the functional effects of IQGAP1 suppression, this paradigm implicates IQGAP1 in the mechanical aspects of TCR signaling.

However, evidence from our rescue experiments suggest that the IQGAP1 C-terminus rescues F-actin levels completely but does not rescue the augmented activation phenotype or TCR signaling. This observation suggests that the negative regulation of signaling by IQGAP1 is independent of its F-actin regulation.

We find that IQGAP1-deficient T cells displayed augmented TCR signaling events as receptor-proximal as LCK phosphorylation, and increased IL-2 and IFN-γ production in $CD8^+$ T cells. A recent study has shown that CD3/CD28-stimulated IQGAP1-depleted $CD8^+$ T cells produced more IFN-γ when compared to wild type cells (50). In this study, the authors demonstrated that IQGAP1 exists in a large cytoplasmic RNA-protein complex containing NFAT, a long intergenic noncoding RNA repressor of NFAT (NRON), and several kinases that regulate NFAT subcellular localization. Importantly, they demonstrated that either depletion of NRON or IQGAP1 led to an increase in the expression of NFAT-dependent cytokines following stimulation. While most IQGAP1 binding partners have been shown to interact with the C-terminal fragment, the N-terminal fragment interacts with ERK1/2 through its WW repeat region (17). Although ERK1/2 are downstream of TCR signaling, these kinases provide a positive feedback loop on TCR signaling through interfering with the interaction of LCK and SHP1 (59). Despite this, we found that expression of the N-terminal fragment of IQGAP1 rescues IL-2 production to wild type levels, while TCR-stimulated signaling remained elevated similar to that seen in IQGAP1-suppressed cells, or those expressing the C-terminal fragment of IQGAP1. It remains possible that the N-terminal region assembles the large RNA-protein complex regulating NFAT nuclear shuttling and enhanced NFAT-mediated transcription, but is incapable of modulating proximal signaling at the level of LCK activation. Clearly, further experiments aimed at elucidating the mechanism by which IQGAP1 integrates TCR-signaling through its dynamic interactions are needed.

We provide evidence that IQGAP1-deficient T cells generate significantly more TCR-stimulated F-actin at the IS and exhibit altered T cell spreading with lamellipodia that are consistently larger than in control T cells. Recent *in vitro* studies from Pelikan-Conchaudron and colleges have demonstrated that the C-terminus of IQGAP1 harbors a calmodulin-regulated F-actin capping region (31) and as such, may control F-actin kinetics during cellular activation. Our results showing that the C-terminus of IQGAP1 is able to rescue the increased F-actin phenotype are consistent with these in vitro findings, such that in the absence of IQGAP1, F-actin filaments continue to grow and generate outward force on the cell membrane. Furthermore, F-actin networks of T cells spreading on CD3-coated coverslips, acutely treated with jasplakinolide, an F-actin stabilizing agent, collapsed inward toward the cSMAC (unpublished observation; JKB and AB), thus F-actin polymerization is the driving force on cell membranes. This is consistent with the idea that heightened F-actin levels could generate an increased outward force on the cell membrane, thus causing the larger lamellipodia. Under normal circumstances, it is possible that IQGAP1 regulation of GTPase activity or its cooperation with Myosin motor proteins may be critical for maintaining balance during TCR-mediated F-actin remodeling (34, 52, 60). Additionally, the IQGAP1 C-terminus interacts with VASP (61), which can positively regulate F-actin nucleation by blocking capping proteins from binding to the barbed-ends of actin filaments (62), as well as Dia1 (32), which can protect barbed-ends from capping proteins (63). Thus, it is possible that the C-terminus of IQGAP1 could sequester these actin regulatory proteins permitting efficient capping. In addition to the C-terminus of IQGAP1, the N-terminus also partially rescued actin dynamics. This might be explained either by the ability of the N-terminus to bind and bundle F-actin via its CH domain (64, 65) or other unknown binding partners. In future studies, it will be important to understand how these various proteins cooperate with IQGAP1 to efficiently regulate lamellipodial dynamics during TCR stimulation.

Taken together, we demonstrate that IQGAP1 acts as a dual negative regulator in T cells, limiting both TCR-mediated activation kinetics and F-actin dynamics via distinct mechanisms. Our study also highlights the complexity of IQGAP1 function in T cells, underscoring the importance of future research aimed at further characterizing the cellular activities of IQGAP proteins, which are likely to illuminate the exact mechanisms by which IQGAP1 can distinctively modulate T cell activation and F-actin dynamics at the IS.

Supplementary Material

Refer to Web version on PubMed Central for supplementary material.

References

1. Campi G, Varma R, Dustin ML. Actin and agonist MHC-peptide complex-dependent T cell receptor microclusters as scaffolds for signaling. J Exp Med. 2005; 202:1031–1036. [PubMed: 16216891]
2. Gomez TS, Billadeau DD. T cell activation and the cytoskeleton: you can't have one without the other. Adv Immunol. 2008; 97:1–64. [PubMed: 18501768]
3. Valitutti S, Dessing M, Aktories K, Gallati H, Lanzavecchia A. Sustained signaling leading to T cell activation results from prolonged T cell receptor occupancy. Role of T cell actin cytoskeleton. J Exp Med. 1995; 181:577–584. [PubMed: 7836913]
4. Holsinger LJ I, Graef A, Swat W, Chi T, Bautista DM, Davidson L, Lewis RS, Alt FW, Crabtree GR. Defects in actin-cap formation in Vav-deficient mice implicate an actin requirement for lymphocyte signal transduction. Curr Biol. 1998; 8:563–572. [PubMed: 9601640]
5. Stinchcombe JC, Majorovits E, Bossi G, Fuller S, Griffiths GM. Centrosome polarization delivers secretory granules to the immunological synapse. Nature. 2006; 443:462–465. [PubMed: 17006514]
6. Nolz JC, Gomez TS, Zhu P, Li S, Medeiros RB, Shimizu Y, Burkhardt JK, Freedman BD, Billadeau DD. The WAVE2 complex regulates actin cytoskeletal reorganization and CRAC-mediated calcium entry during T cell activation. Curr Biol. 2006; 16:24–34. [PubMed: 16401421]
7. Nolz JC, Fernandez-Zapico ME, Billadeau DD. TCR/CD28-stimulated actin dynamics are required for NFAT1-mediated transcription of c-rel leading to CD28 response element activation. J Immunol. 2007; 179:1104–1112. [PubMed: 17617603]
8. Suetsugu S, Miki H, Takenawa T. Identification of two human WAVE/SCAR homologues as general actin regulatory molecules which associate with the Arp2/3 complex. Biochem Biophys Res Commun. 1999; 260:296–302. [PubMed: 10381382]
9. Huang Y, Burkhardt JK. T-cell-receptor-dependent actin regulatory mechanisms. J Cell Sci. 2007; 120:723–730. [PubMed: 17314246]
10. Zeng R, Cannon JL, Abraham RT, Way M, Billadeau DD, Bubeck-Wardenberg J, Burkhardt JK. SLP-76 coordinates Nck-dependent Wiskott-Aldrich syndrome protein recruitment with Vav-1/Cdc42-dependent Wiskott-Aldrich syndrome protein activation at the T cell-APC contact site. J Immunol. 2003; 171:1360–1368. [PubMed: 12874226]
11. Snapper SB, Rosen FS. The Wiskott-Aldrich syndrome protein (WASP): roles in signaling and cytoskeletal organization. Annu Rev Immunol. 1999; 17:905–929. [PubMed: 10358777]
12. Gomez TS, McCarney SD, Carrizosa E, Labno CM, Comiskey EO, Nolz JC, Zhu P, Freedman BD, Clark MR, Rawlings DJ, Billadeau DD, Burkhardt JK. HS1 functions as an essential actin-regulatory adaptor protein at the immune synapse. Immunity. 2006; 24:741–752. [PubMed: 16782030]
13. Brandt DT, Grosse R. Get to grips: steering local actin dynamics with IQGAPs. EMBO Rep. 2007; 8:1019–1023. [PubMed: 17972901]
14. White CD, Brown MD, Sacks DB. IQGAPs in cancer: a family of scaffold proteins underlying tumorigenesis. FEBS Lett. 2009; 583:1817–1824. [PubMed: 19433088]
15. Weissbach L, Settleman J, Kalady MF, Snijders AJ, Murthy AE, Yan YX, Bernards A. Identification of a human rasGAP-related protein containing calmodulin-binding motifs. J Biol Chem. 1994; 269:20517–20521. [PubMed: 8051149]

16. Noritake J, Watanabe T, Sato K, Wang S, Kaibuchi K. IQGAP1: a key regulator of adhesion and migration. J Cell Sci. 2005; 118:2085–2092. [PubMed: 15890984]

17. Roy M, Li Z, Sacks DB. IQGAP1 binds ERK2 and modulates its activity. J Biol Chem. 2004; 279:17329–17337. [PubMed: 14970219]

18. Roy M, Li Z, Sacks DB. IQGAP1 is a scaffold for mitogen-activated protein kinase signaling. Mol Cell Biol. 2005; 25:7940–7952. [PubMed: 16135787]

19. Ren JG, Li Z, Sacks DB. IQGAP1 modulates activation of B-Raf. Proc Natl Acad Sci USA. 2007; 104:10465–10469. [PubMed: 17563371]

20. McCallum SJ, Wu WJ, Cerione RA. Identification of a putative effector for Cdc42Hs with high sequence similarity to the RasGAP-related protein IQGAP1 and a Cdc42Hs binding partner with similarity to IQGAP2. J Biol Chem. 1996; 271:21732–21737. [PubMed: 8702968]

21. Kuroda S, Fukata M, Kobayashi K, Nakafuku M, Nomura N, Iwamatsu A, Kaibuchi K. Identification of IQGAP as a putative target for the small GTPases, Cdc42 and Rac1. J Biol Chem. 1996; 271:23363–23367. [PubMed: 8798539]

22. Hart MJ, Callow MG, Souza B, Polakis P. IQGAP1, a calmodulin-binding protein with a rasGAP-related domain, is a potential effector for cdc42Hs. EMBO J. 1996; 15:2997–3005. [PubMed: 8670801]

23. Yamaoka-Tojo M, Ushio-Fukai M, Hilenski L, Dikalov SI, Chen YE, Tojo T, Fukai T, Fujimoto M, Patrushev NA, Wang N, Kontos CD, Bloom GS, Alexander RW. IQGAP1, a novel vascular endothelial growth factor receptor binding protein, is involved in reactive oxygen species--dependent endothelial migration and proliferation. Circ Res. 2004; 95:276–283. [PubMed: 15217908]

24. Watanabe T, Wang S, Noritake J, Sato K, Fukata M, Takefuji M, Nakagawa M, Izumi N, Akiyama T, Kaibuchi K. Interaction with IQGAP1 links APC to Rac1, Cdc42, and actin filaments during cell polarization and migration. Dev Cell. 2004; 7:871–883. [PubMed: 15572129]

25. Watanabe T, Noritake J, Kaibuchi K. Roles of IQGAP1 in cell polarization and migration. Novartis Found Symp. 2005; 269:92–101. discussion 101–5, 223–30. [PubMed: 16355537]

26. Mataraza JM, Briggs MW, Li Z, Entwistle A, Ridley AJ, Sacks DB. IQGAP1 promotes cell motility and invasion. J Biol Chem. 2003; 278:41237–41245. [PubMed: 12900413]

27. Li Z, Kim SH, Higgins JM, Brenner MB, Sacks DB. IQGAP1 and calmodulin modulate E-cadherin function. J Biol Chem. 1999; 274:37885–37892. [PubMed: 10608854]

28. Drees F, Pokutta S, Yamada S, Nelson WJ, Weis WI. Alpha-catenin is a molecular switch that binds E-cadherin-beta-catenin and regulates actin-filament assembly. Cell. 2005; 123:903–915. [PubMed: 16325583]

29. Verma S, Shewan AM, Scott JA, Helwani FM, den Elzen NR, Miki H, Takenawa T, Yap AS. Arp2/3 activity is necessary for efficient formation of E-cadherin adhesive contacts. J Biol Chem. 2004; 279:34062–34070. [PubMed: 15159390]

30. Sahai E, Marshall CJ. ROCK and Dia have opposing effects on adherens junctions downstream of Rho. Nat Cell Biol. 2002; 4:408–415. [PubMed: 11992112]

31. Pelikan-Conchaudron A, Le Clainche C, Didry D, Carlier MF. The IQGAP1 protein is a calmodulin-regulated barbed end capper of actin filaments: possible implications in its function in cell migration. J Biol Chem. 2011; 286:35119–35128. [PubMed: 21730051]

32. Brandt DT, Marion S, Griffiths G, Watanabe T, Kaibuchi K, Grosse R. Dia1 and IQGAP1 interact in cell migration and phagocytic cup formation. J Cell Biol. 2007; 178:193–200. [PubMed: 17620407]

33. Le Clainche C, Schlaepfer D, Ferrari A, Klingauf M, Grohmanova K, Veligodskiy A, Didry D, Le D, Egile C, Carlier MF, Kroschewski R. IQGAP1 stimulates actin assembly through the N-WASP-Arp2/3 pathway. J Biol Chem. 2007; 282:426–435. [PubMed: 17085436]

34. Weissbach L, Bernards A, Herion DW. Binding of myosin essential light chain to the cytoskeleton-associated protein IQGAP1. Biochem Biophys Res Commun. 1998; 251:269–276. [PubMed: 9790945]

35. Fukata M, Watanabe T, Noritake J, Nakagawa M, Yamaga M, Kuroda S, Matsuura Y, Iwamatsu A, Perez F, Kaibuchi K. Rac1 and Cdc42 capture microtubules through IQGAP1 and CLIP-170. Cell. 2002; 109:873–885. [PubMed: 12110184]

36. Lansbergen G, Akhmanova A. Microtubule plus end: a hub of cellular activities. Traffic. 2006; 7:499–507. [PubMed: 16643273]
37. Sedwick CE, Morgan MM, Jusino L, Cannon JL, Miller J, Burkhardt JK. TCR, LFA-1, and CD28 play unique and complementary roles in signaling T cell cytoskeletal reorganization. J Immunol. 1999; 162:1367–1375. [PubMed: 9973391]
38. Williams BL, Schreiber KL, Zhang W, Wange RL, Samelson LE, Leibson PJ, Abraham RT. Genetic evidence for differential coupling of Syk family kinases to the T-cell receptor: reconstitution studies in a ZAP-70-deficient Jurkat T-cell line. Mol Cell Biol. 1998; 18:1388–1399. [PubMed: 9488454]
39. Karnitz L, Sutor SL, Torigoe T, Reed JC, Bell MP, McKean DJ, Leibson PJ, Abraham RT. Effects of p56lck deficiency on the growth and cytolytic effector function of an interleukin-2-dependent cytotoxic T-cell line. Mol Cell Biol. 1992; 12:4521–4530. [PubMed: 1406641]
40. Gil D, Schrum AG, Daniels MA, Palmer E. A role for CD8 in the developmental tuning of antigen recognition and CD3 conformational change. J Immunol. 2008; 180:3900–3909. [PubMed: 18322198]
41. Gomez TS, Hamann MJ, McCarney S, Savoy DN, Lubking CM, Heldebrant MP, Labno CM, McKean DJ, McNiven MA, Burkhardt JK, Billadeau DD. Dynamin 2 regulates T cell activation by controlling actin polymerization at the immunological synapse. Nat Immunol. 2005; 6:261–270. [PubMed: 15696170]
42. Gomez TS, Kumar K, Medeiros RB, Shimizu Y, Leibson PJ, Billadeau DD. Formins regulate the actin-related protein 2/3 complex-independent polarization of the centrosome to the immunological synapse. Immunity. 2007; 26:177–190. [PubMed: 17306570]
43. Arneson LN, Segovis CM, Gomez TS, Schoon RA, Dick CJ, Lou Z, Billadeau DD, Leibson PJ. Dynamin 2 regulates granule exocytosis during NK cell-mediated cytotoxicity. J Immunol. 2008; 181:6995–7001. [PubMed: 18981119]
44. Li S, Wang Q, Chakladar A, Bronson RT, Bernards A. Gastric hyperplasia in mice lacking the putative Cdc42 effector IQGAP1. Mol Cell Biol. 2000; 20:697–701. [PubMed: 10611248]
45. Windebank KP, Abraham RT, Powis G, Olsen RA, Barna TJ, Leibson PJ. Signal transduction during human natural killer cell activation: inositol phosphate generation and regulation by cyclic AMP. J Immunol. 1988; 141:3951–3957. [PubMed: 2846696]
46. Gomez TS, Billadeau DD. A FAM21-containing WASH complex regulates retromer-dependent sorting. Dev Cell. 2009; 17:699–711. [PubMed: 19922874]
47. Zhang JS, Koenig A, Harrison A, Ugolkov AV, Fernandez-Zapico ME, Couch FJ, Billadeau DD. Mutant K-Ras increases GSK-3β gene expression via an ETS-p300 transcriptional complex in pancreatic cancer. Oncogene. 2011; 30:3705–3715. [PubMed: 21441955]
48. Bunnell SC V, Barr A, Fuller CL, Samelson LE. High-resolution multicolor imaging of dynamic signaling complexes in T cells stimulated by planar substrates. Sci STKE. 2003; 2003:PL8. [PubMed: 12684528]
49. Schmidt VA, Chiariello CS, Capilla E, Miller F, Bahou WF. Development of hepatocellular carcinoma in Iqgap2-deficient mice is IQGAP1 dependent. Mol Cell Biol. 2008; 28:1489–1502. [PubMed: 18180285]
50. Sharma S, Findlay GM, Bandukwala HS, Oberdoerffer S, Baust B, Li Z, Schmidt V, Hogan PG, Sacks DB, Rao A. Dephosphorylation of the nuclear factor of activated T cells (NFAT) transcription factor is regulated by an RNA-protein scaffold complex. Proc Natl Acad Sci USA. 2011; 108:11381–11386. [PubMed: 21709260]
51. Bunnell SC, Kapoor V, Trible RP, Zhang W, Samelson LE. Dynamic actin polymerization drives T cell receptor-induced spreading: a role for the signal transduction adaptor LAT. Immunity. 2001; 14:315–329. [PubMed: 11290340]
52. Brown MD, Sacks DB. IQGAP1 in cellular signaling: bridging the GAP. Trends Cell Biol. 2006; 16:242–249. [PubMed: 16595175]
53. Kanwar N, Wilkins JA. IQGAP1 involvement in MTOC and granule polarization in NK-cell cytotoxicity. Eur J Immunol. 2011; 41:2763–2773. [PubMed: 21681737]

54. Rak GD, Mace EM, Banerjee PP, Svitkina T, Orange JS. Natural killer cell lytic granule secretion occurs through a pervasive actin network at the immune synapse. PLoS Biol. 2011; 9:e1001151. [PubMed: 21931536]
55. Sanborn KB, Rak GD, Maru SY, Demers K, Difeo A, Martignetti JA, Betts MR, Favier R, Banerjee PP, Orange JS. Myosin IIA associates with NK cell lytic granules to enable their interaction with F-actin and function at the immunological synapse. J Immunol. 2009; 182:6969–6984. [PubMed: 19454694]
56. Lyubchenko TA, Wurth GA, Zweifach A. The actin cytoskeleton and cytotoxic T lymphocytes: evidence for multiple roles that could affect granule exocytosis-dependent target cell killing. J Physiol (Lond). 2003; 547:835–847. [PubMed: 12576500]
57. Beemiller P, Krummel MF. Mediation of T-cell activation by actin meshworks. Cold Spring Harb Perspect Biol. 2010; 2:a002444. [PubMed: 20702599]
58. Li YC, Chen BM, Wu PC, Cheng TL, Kao LS, Tao MH, Lieber A, Roffler SR. Cutting Edge: mechanical forces acting on T cells immobilized via the TCR complex can trigger TCR signaling. J Immunol. 2010; 184:5959–5963. [PubMed: 20435924]
59. Acuto O, Di Bartolo V, Michel F. Tailoring T-cell receptor signals by proximal negative feedback mechanisms. Nat Rev Immunol. 2008; 8:699–712. [PubMed: 18728635]
60. Pathmanathan S, Hamilton E, Atcheson E, Timson DJ. The interaction of IQGAPs with calmodulin-like proteins. Biochem Soc Trans. 2011; 39:694–699. [PubMed: 21428964]
61. Routray C, Liu C, Yaqoob U, Billadeau DD, Bloch KD, Kaibuchi K, Shah VH, Kang N. Protein kinase G signaling disrupts Rac1-dependent focal adhesion assembly in liver specific pericytes. Am J Physiol, Cell Physiol. 2011; 301:C66–74. [PubMed: 21451103]
62. Bear JE, Svitkina TM, Krause M, Schafer DA, Loureiro JJ, Strasser GA, Maly IV, Chaga OY, Cooper JA, Borisy GG, Gertler FB. Antagonism between Ena/VASP proteins and actin filament capping regulates fibroblast motility. Cell. 2002; 109:509–521. [PubMed: 12086607]
63. Paul AS, Pollard TD. Review of the mechanism of processive actin filament elongation by formins. Cell Motil Cytoskeleton. 2009; 66:606–617. [PubMed: 19459187]
64. Umemoto R, Nishida N, Ogino S, Shimada I. NMR structure of the calponin homology domain of human IQGAP1 and its implications for the actin recognition mode. J Biomol NMR. 2010; 48:59–64. [PubMed: 20644981]
65. Mateer SC, Morris LE, Cromer DA, Benseñor LB, Bloom GS. Actin filament binding by a monomeric IQGAP1 fragment with a single calponin homology domain. Cell Motil Cytoskeleton. 2004; 58:231–241. [PubMed: 15236354]

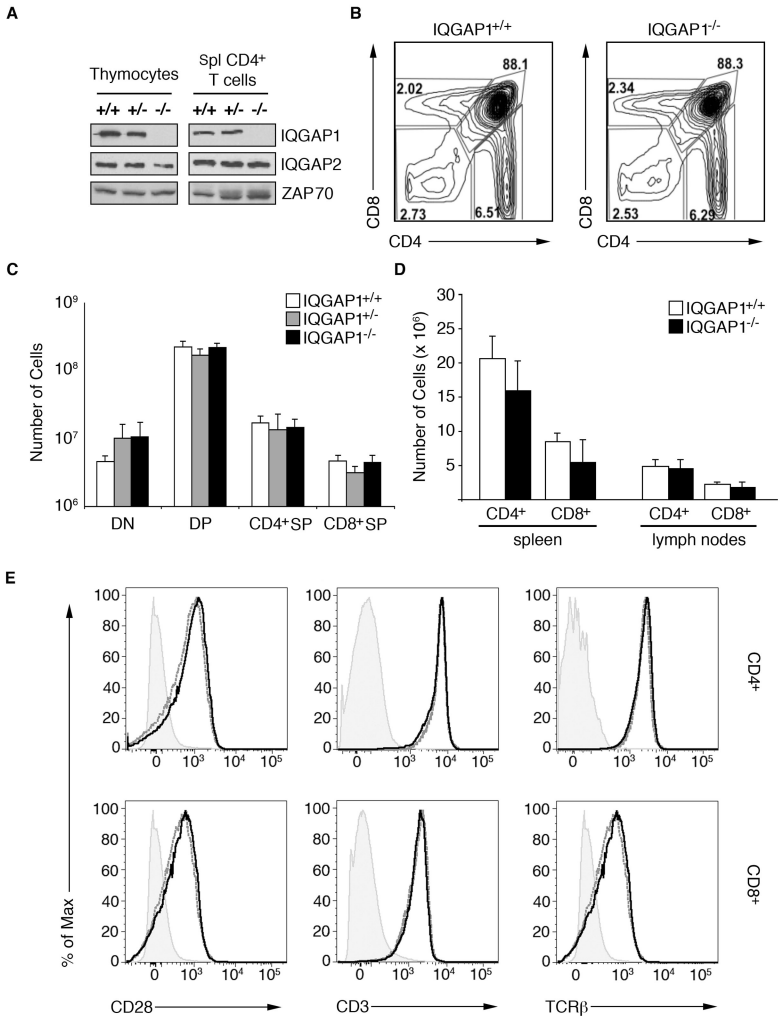

Figure 1.

Thymocyte development and peripheral T cell numbers are normal in IQGAP1$^{-/-}$ mice. (**A**) Thymocyte and splenic CD4^{+} T cell lysates from IQGAP1$^{+/+}$, IQGAP1$^{+/-}$, or IQGAP1$^{-/-}$ mice were immunoblotted as indicated. (**B**) Flow cytometric analysis of CD4 and CD8 expression on thymocytes of IQGAP1$^{+/+}$ and IQGAP1$^{-/-}$ mice. (**C**) Total cell numbers of each population are depicted (DN-double negative thymocytes, DP-double positive thymocytes, CD4+SP-single positive CD4^{+} thymocytes, and CD8^{+}SP- single positive CD8^{+} thymocytes). (**D**) Flow cytometric analysis of CD4 and CD8 expression on splenocytes and lymphocytes from IQGAP1$^{+/+}$ or IQGAP1$^{-/-}$mice. Total cell number is depicted. (n = 5). (**E**) Cell surface receptor levels are unchanged in IQGAP1$^{-/-}$ T cells. Flow cytometric analysis of the expression of receptors on CD4+ and CD8+ splenocytes. Gray dotted line, IQGAP1$^{-/-}$; Black dotted line, IQGAP1$^{+/+}$; Light gray shading, IgG control. Data depicted as mean ±SD.

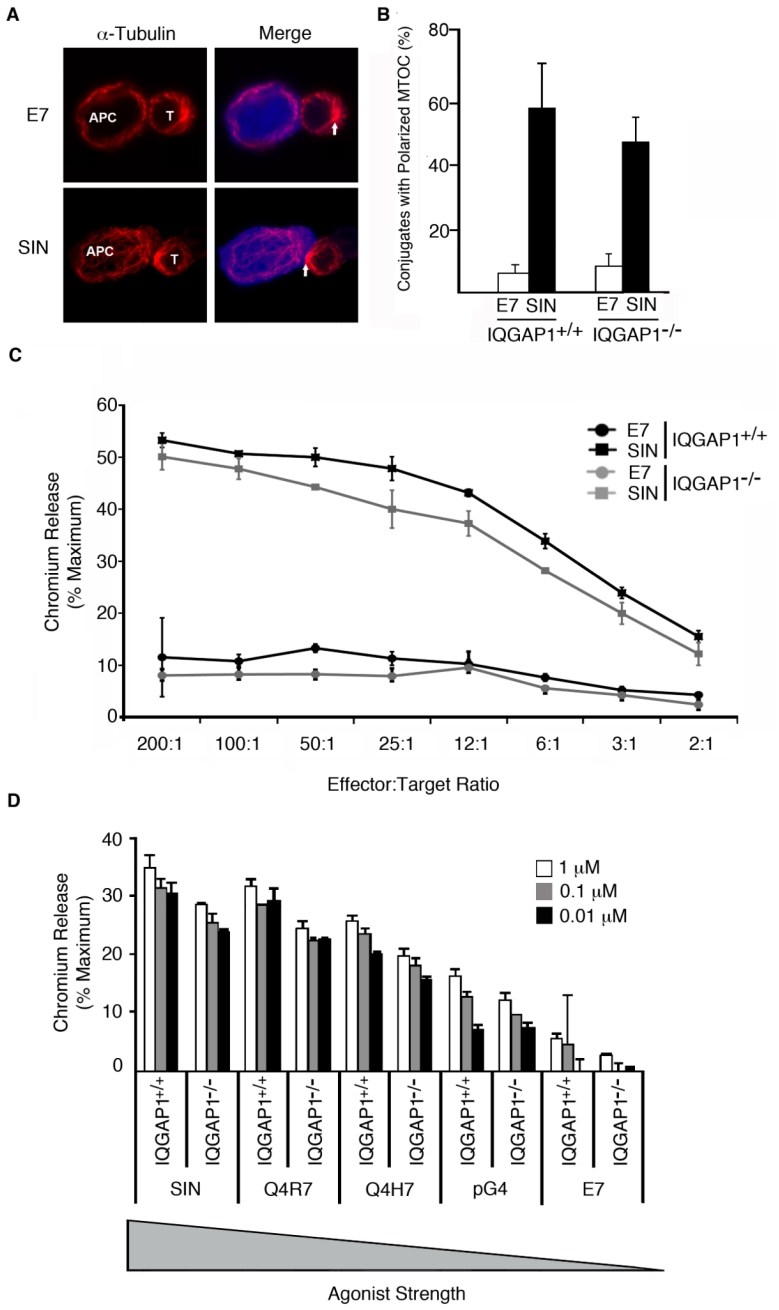

Figure 2.

Loss of IQGAP1 does not affect MTOC polarization or $CD8^+$ T cell cytotoxicity. (**A** and **B**) EL-4 cells were loaded with SIN-SIINFEKL or E7-nonspecific peptides and conjugates were formed with $IQGAP1^{+/+}$ or $IQGAP1^{-/-}$ OT-I T cells. Conjugates were bound to poly-L-Lysine coated coverslips, fixed, and stained with α-tubulin. Polarization of the MTOC was assessed. Representative pictures of MTOC polarization are shown in (A) and quantitative analysis in (B). Data shown is representative of three independent experiments. (**C** and **D**) $IQGAP1^{+/+}$ or $IQGAP1^{-/-}CD8^+$ T cells were tested for cytotoxicity against SIN-/E7-/APL-loaded EL-4 cells. Data shown is representative of two independent experiments. Error bars represent ±SD. APL=Altered Peptide Ligand.

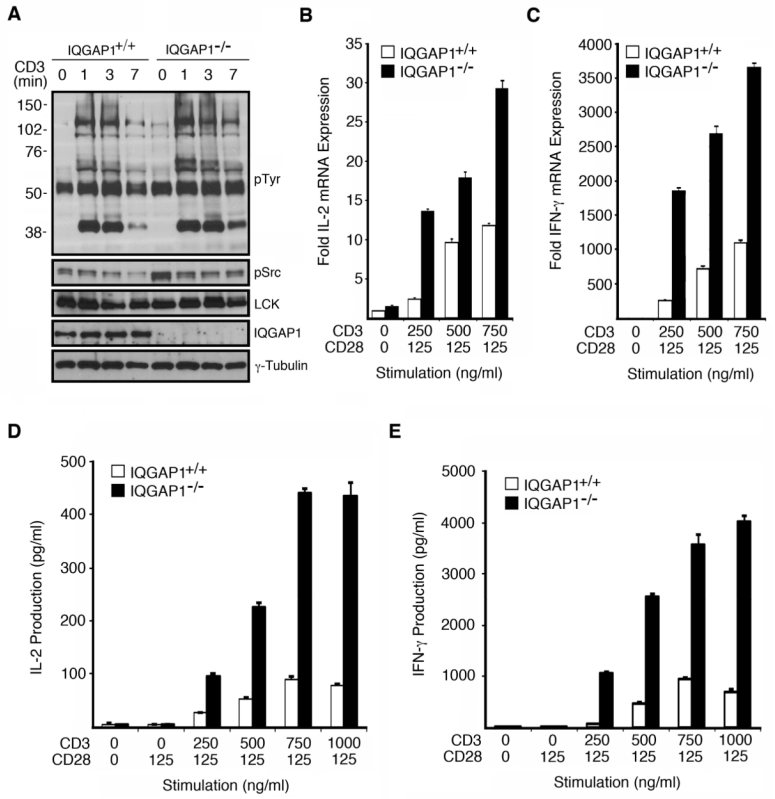

Figure 3.

IQGAP1-deficient T cells have enhanced TCR-mediated signaling leading to increased cytokine production. (**A**) OT-I CD8$^+$ T cells from IQGAP1$^{-/-}$ or IQGAP1$^{+/+}$ mice were labeled with anti-CD3 and crosslinked with goat anti-hamster IgG over the indicated time course. Whole cell lysates were resolved by SDS-PAGE and immunoblotted as indicated. Data shown is representative of three independent experiments. (**B** and **C**) OT-I CD8$^+$ T cells from IQGAP1$^{-/-}$ or IQGAP1$^{+/+}$ mice were stimulated overnight with plate bound anti-CD3 and soluble anti-CD28 at the indicated concentrations, and quantitative RT-PCR was performed for IL-2 (B) and IFN-γ (C) gene expression. Results were normalized to the large ribosomal protein, RPLPO, gene expression. (**D** and **E**) OT-I CD8$^+$ T cells from IQGAP1$^{-/-}$ or IQGAP1$^{+/+}$ mice were stimulated overnight with plate bound anti-CD3 and soluble anti-CD28 at the indicated concentrations, and secreted IL-2 (D) and IFN-γ (E) was measured by ELISA. Data shown is representative of two independent experiments. Bars represent mean ±SD.

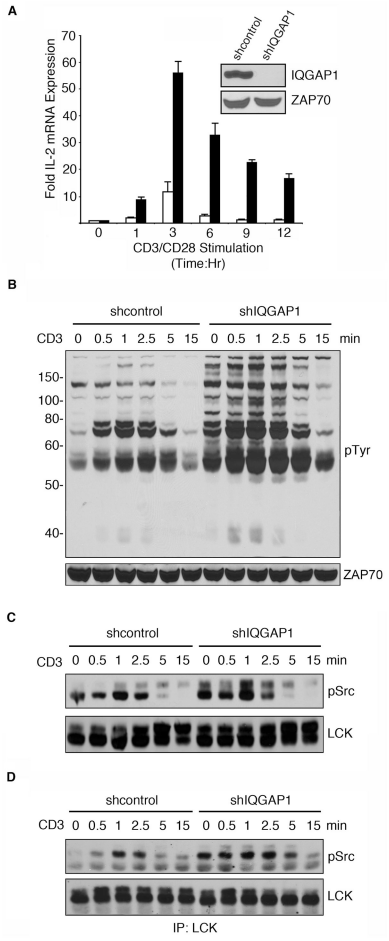

Figure 4.

IQGAP1-deficient T cells have enhanced TCR-mediated signaling. (**A–D**) Jurkat T cells were transfected with shcontrol or shIQGAP1 and stimulated with soluble anti-CD3, anti-CD28 and goat-anti-mouse IgG for the indicated times. (**A**) qRT-PCR was performed to determine the amount of IL-2 mRNA. Results are normalized to RPLPO. (**B**) Whole cell lysates were resolved by SDS-PAGE and immunoblotted with (B) phospho-tyrosine antibody 4G10 and ZAP-70 as a loading control, or (C) pSrc(Y416) and total LCK. (**D**) Jurkat cells were stimulated and LCK was immunoprecipitated and immunoblotted with pSrc(Y416). Data shown is representative of three independent experiments. Bars represent mean ±SD.

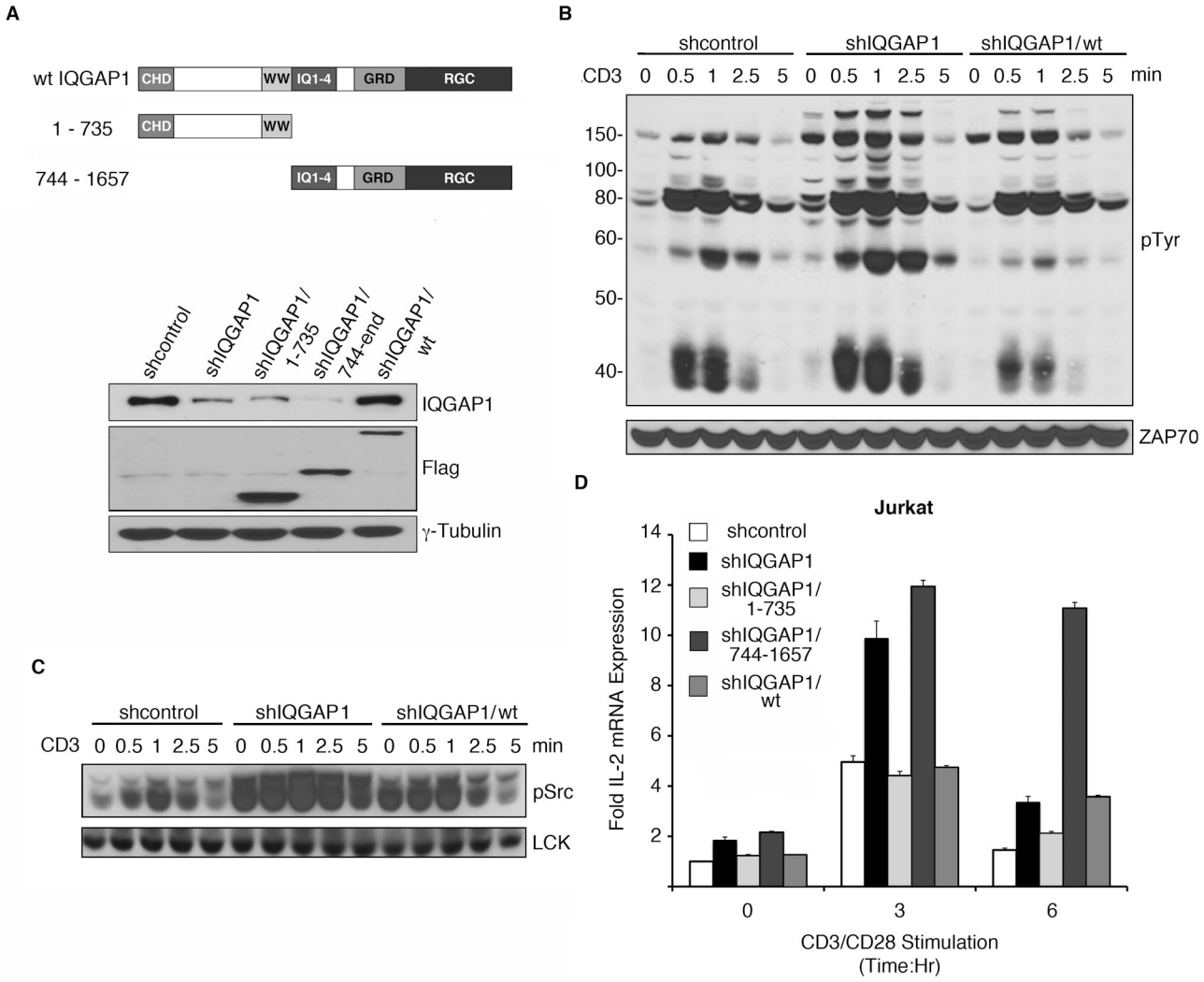

Figure 5.

IQGAP1 domains differentially affect T cell signaling. (**A**) IQGAP1 mutants used in suppression/reconstitution studies (upper panel) and representative immunoblot of IQGAP1 suppression and re-expression of wild type and truncated proteins (lower panel). (**B** and **C**) Jurkat T cells were transfected with the indicated suppression vectors and stimulated with anti-CD3/goat anti-mouse IgG over the indicated time course. Whole cell lysates were resolved by SDS-PAGE and immunoblotted with the indicated antibodies. (**D**) Jurkat T cells were transfected with the indicated suppression/re-expression vectors described in (A). Quantitative RT-PCR was performed to analyze IL-2 mRNA (normalized to RPLPO) produced over the indicated time course. Data shown is representative of three independent experiments. Error bars show mean ±SD.

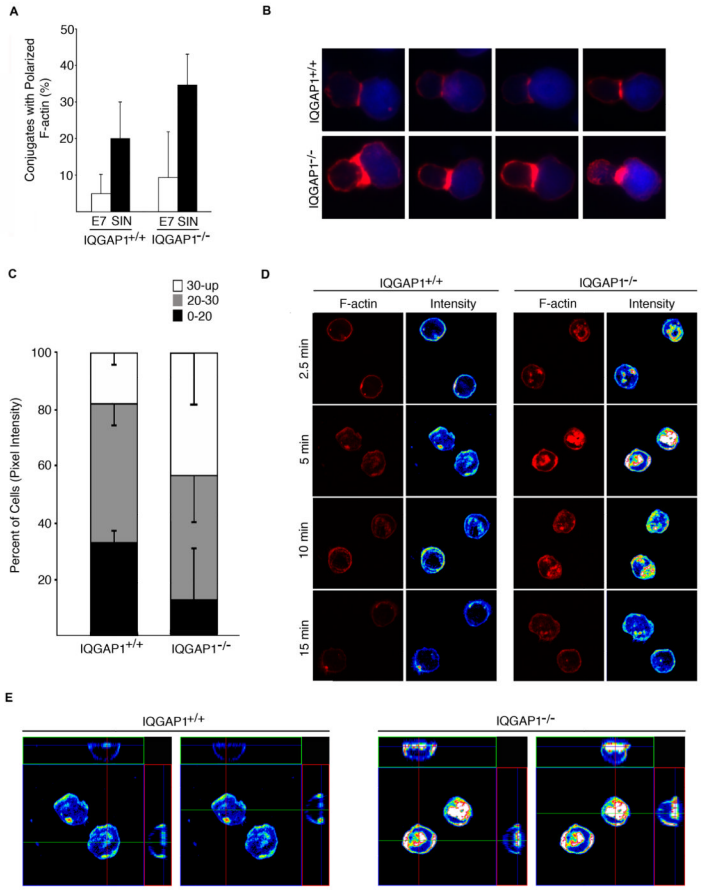

Figure 6.

F-actin is increased in IQGAP1$^{-/-}$ T cells. (**A–C**) EL-4 cells were loaded with SIN or E7 peptides and conjugated with OT-I T TCR transgenic T cells obtained from IQGAP1$^{+/+}$ or IQGAP1$^{-/-}$ mice. Conjugates were bound to poly-L-lysine coated coverslips, fixed, and stained with rhodamine-phalloidin. Quantitative analysis of the percentage of cells with polarized F-actin is shown in (**A**) and representative pictures in (**B**). Pictures were taken at the same intensity/time of exposure. (**C**) The amount of polarized F-actin per cell was quantified using average pixel intensity. (**D** and **E**) IQGAP1$^{+/+}$ or IQGAP1$^{-/-}$ CD8^{+} T cells were allowed to settle onto Poly-L-lysine coated coverslips that had also been coated with anti-CD3 for the indicated time course. Cells were stained with rhodamine-conjugated phalloidin and imaged with a confocal microscope. F-actin and pseudo-coloring for F-actin intensity are shown. Representative pictures are shown in (D) and 3D reconstruction of spreading cells at 5 minutes post-stimulation are shown in (E).

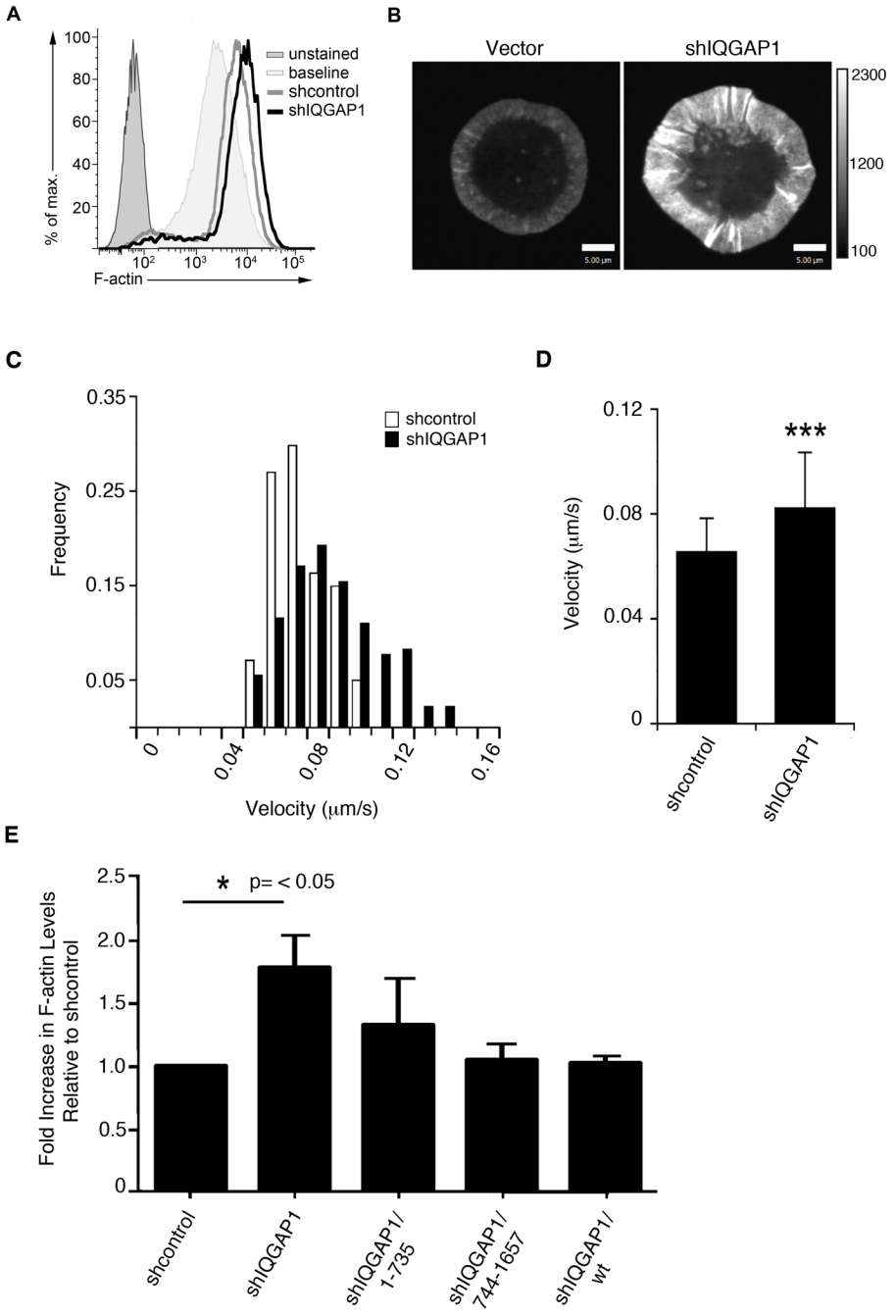

Figure 7.

IQGAP1 negatively regulates F-actin accumulation at the IS. (**A**) Jurkat T cells were transfected with shRNA vectors and stimulated with anti-CD3/anti-CD28. Cells were fixed, permeabilized, stained with FITC-phalloidin, and analyzed by flow cytometry. Data shown is a representative flow plot. Baseline = 0 min stimulation, shControl and shIQGAP1 = 1 min post anti-CD3/CD28 ligation (n=3). (**B**) Jurkat T cells stably expressing GFP-actin were transfected with the indicated suppression plasmids. Cells were harvested 72-hr post electroporation and knockdown was confirmed by Western blot analysis. Cells were imaged while interacting with OKT3-coated cover glasses. Z stacks were collected just above the glass, using the same exposure settings for all cells. Representative still images are shown as

extended projections. Intensity is shown as a grayscale gradient. Scale bars represent 5.0 μm. (**C** and **D**) Velocity of F-actin flow was analyzed using kymographs drawn along the radii of the IS from cell populations in (B). Data represent mean ± SD of at least 140 kymographs from at least 36 cells, pooled from two independent experiments. ***$p<0.001$. (**E**) Jurkat T cells were transfected with IQGAP1 mutants and F-actin content was analyzed as in (A). Results were normalized to shcontrol (n=5). Error bars represent ±SD.